Polyunsaturated fatty acids inhibit kv1.4 by interacting with positively charged extracellular pore residues

DOI:
10.1152/ajpcell.00277.2015

Document Version
Accepted author manuscript

Polyunsaturated fatty acids inhibit $K_v1.4$ by interacting with positively-charged extracellular pore residues

Running title: PUFAs and $K_v1.4$

N.E. Farag[1,4#], D. Jeong[2#], T. Claydon[2]*, J. Warwicker[3]* and M.R. Boyett[1]*

*Joint senior authors

[#]Joint first authors

[1]Cardiovascular Medicine, School of Medicine, University of Manchester, Core Technology Facility, 46 Grafton Street, Manchester M13 9NT, UK

[2]Department of Biomedical Physiology and Kinesiology, Simon Fraser University, Burnaby, British Columbia, V5A 1S6, Canada

[3]Manchester Institute of Biotechnology, The University of Manchester, 131 Princess Street, Manchester, M1 7DN, United Kingdom

[4]Current address: Department of Physiology, Faculty of Medicine, Suez Canal University

Correspondence to: Professor M.R. Boyett

Tel: +44-161-275-1192 E-mail: mark.boyett@manchester.ac.uk

Keywords

Potassium channels; PUFAs; inactivation

Abstract

Polyunsaturated fatty acids (PUFAs) modulate voltage-gated K^+ channel inactivation by an unknown site and mechanism. Effects of ω-6 and ω-3 PUFAs were investigated on the heterologously expressed $K_v1.4$ channel. PUFAs inhibited wild-type $K_v1.4$ during repetitive pulsing as a result of slowing of recovery from inactivation. In a mutant $K_v1.4$ channel lacking N-type inactivation, PUFAs reversibly enhanced C-type inactivation (K_D, 15-43 μM). C-type inactivation was affected by extracellular H^+ and K^+ as well as PUFAs and there was an interaction among the three: the effect of PUFAs was reversed during acidosis and abolished on raising K^+. Replacement of two positively-charged residues in the extracellular pore (H508 and K532) abolished the effects of the PUFAs (and extracellular H^+ and K^+) on C-type inactivation, but had no effect on the lipoelectric modulation of voltage sensor activation, suggesting two separable interaction sites/mechanisms of action of PUFAs. Charge calculations suggest that the acidic head group of the PUFAs raises the pK_a of H508 and this reduces the K^+ occupancy of the selectivity filter, stabilising the C-type inactivated state.

Introduction

Neuronal electrical properties are shaped in large part by the action of voltage-gated K^+ channels. They contribute to postsynaptic potentials, action potential firing and propagation, neurotransmitter release, and even learning and memory (37). One of the three most abundant K_v1 channels expressed in the mammalian brain is $K_v1.4$, a transient outward K^+ channel (47). $K_v1.4$ is concentrated along axons and within axon terminals (47) and this critical position allows it to regulate depolarization of the axon terminals and, therefore, neurotransmitter release. Voltage-gated K^+ channels also play an important role in the heart. $K_v1.4$ is expressed in the heart and it contributes to the transient outward K^+ current, which

underlies the early repolarization phase of the cardiac action potential and helps determine action potential duration (8). In the heart, the transient outward K^+ current plays an important role in the development of the repolarization dispersion that occurs during acute myocardial ischaemia - this predisposes to the development of ventricular tachyarrhythmias (27).

Polyunsaturated fatty acids (PUFAs) play an important physiological and pathophysiological role in both the brain and heart. The ω-6 PUFA, arachidonic acid (20:4n6), and two major ω-3 PUFAs, eicosapentaenoic acid (20:5n3, EPA) and docosahexaenoic acid (22:6n3, DHA), are crucial components of neural membranes. ω-6 and ω-3 PUFAs are needed for brain growth and functional development during foetal life and infancy (15) and epidemiological data indicate that low ω-3 PUFA intake is a risk factor for Alzheimer's disease (10). There is evidence that dietary ω-3 PUFAs, abundant in marine organisms, may reduce the development of cardiac arrhythmias and the mortality rate following coronary heart disease in humans (27) and in animal models (4). The concentration of unbound arachidonic acid in normal human serum is small (0.05-0.5 μM), but the concentration is raised in various diseases including diabetes and leukaemia (35). In addition, in the brain and heart, the concentration of arachidonic acid rises greatly in ischaemia and after seizures (35). For example, in the heart, it is known that myocardial ischaemia can result in hydrolysis of phospholipids and release of arachidonic acid from the cell membrane by the activity of phospholipase A_2 (3). In the ischaemic heart, arachidonic acid also could accumulate as a result of hormonal activation or the failure of fatty acid oxidation (3). The concentration of ω-3 PUFAs in plasma of humans consuming a regular Western diet ranges from 8 to 12 μM, but consuming moderate to high fish intake for several months can raise plasma ω-3 PUFA concentrations to 200–400 μM (42).

The PUFAs inhibit the transient outward K^+ current both in the brain and the heart (see Discussion) and the aim of this study was to investigate the mechanism of action of ω-6

and ω-3 PUFAs on K_v1.4. A number of previous studies have investigated the effects of PUFAs on K_v channels (21; 23; 34; 40; 43; 48; 48); however the site and mechanism of action of PUFAs are uncertain. DHA inhibits K_v1.2 channels, an effect that has been ascribed to external block (40), while linoleic acid modulates K_v2.1 from the extracellular side (34). Likewise, the inhibitory effects of α-linolenic acid, AA, DHA, and linoleic acid on K_v1.5 were shown to be externally mediated (21; 23; 34). On the other hand, anandamide blocked K_v1.5 channels significantly faster when applied intracellularly and is competed away for TEA, suggesting intracellular pore block (36). In contrast to this PUFA-induced inhibition, lower concentrations of PUFAs *increased* peak current amplitude in K_v1.1 (17) and K_v1.5 (23). Enhanced activation has also been described in K_v1.2 (40) with DHA, K_v11.1 with AA and DHA (19), and K_v1.5 and K_v2.1 with linoleic acid (34). More recent studies in *Shaker* potassium channels, show that PUFAs induce a leftward shift of the voltage dependence of activation by several mV (7). This 'lipoelectric' effect stabilises the open state of Kv channels, and was recently shown to rescue wild-type like function in an arrhythmia-inducing mutant Kv7.1 channel in which the open-state of the channel was destabilised by the mutation (29). The underlying mechanism is the best characterised action of PUFAs in K_v channels, and has been shown to be due to electrostatic interactions of the PUFA head-group with the voltage sensor of the channel during its final activation transition (6; 7).

Oliver et al., described the conversion of non-A-type channels to rapidly inactivating channels in response to externally applied PUFAs (39). The authors demonstrated that inactivation was dramatically enhanced by PUFAs and that the effect was mediated by a PUFA-induced collapse of the outer mouth of the pore that induced stabilisation of the C-type inactivated state, and was not mediated by intracellular block of the pore. Despite characterisation of the effects of PUFAs on K_v channel inactivation, neither the site of action of PUFAs, nor the mechanism by which PUFAs stabilise the collapsed, inactivated,

configuration of the outer pore is known. Here, we studied the action of the ω-6 PUFA, arachidonic acid, and the ω-3 PUFAs, EPA and DHA on Kv1.4 channel function and demonstrate that the PUFA-induced inactivation is mediated by an outer pore histidine residue, whose charge modification by the PUFA head-group destabilises K^+ occupancy within the outer pore and that this stabilises the inactivated state. We show that this underlies what was observed as an apparent extracellular block of K_v1.4 channels. Moreover, our mutagenesis dissects the effect of PUFAs from the lipoelectric effect and demonstrates that there are at least two separable effects of external PUFAs in Kv channels.

Materials and Methods

Molecular biology

Experiments were carried out on: wild-type K_v1.4 (rat); a truncated version of K_v1.4 (ferret), K_v1.4 Δ2-146, lacking rapid N-type inactivation; and two mutants of the truncated channel, K_v1.4 Δ2-146 H508C and K_v1.4 Δ2-146 K532C (13). Since rat and ferret K_v1.4 channel isoforms exhibit very high sequence homology (only 14 of the 654 amino acids differ; one divergence in the transmembrane core of the channel and 13, mostly conservative, differences in the cytoplasmic domains), and both display rapid N-type inactivation and slower C-type inactivation, our interpretations from data with either clone also likely hold for the other. In all cases, vectors (pBluescript $SKII^+$ for rat K_v1.4 and pBluescript SK^- for ferret K_v1.4) containing the cDNA sequences were linearised with a restriction endonuclease (*Eco* RI for rat K_v1.4 and *Asp* 718 for ferret K_v1.4) and cRNA was prepared from these templates with either T7 (rat K_v1.4) or T3 (ferret K_v1.4) RNA polymerase (Stratagene). Transcribed RNA was diluted in diethyl pyrocarbonate (DEPC) treated water to a final concentration of 50 ng/μl (rat K_v1.4) or 100 ng/μl (ferret K_v1.4).

Electrophysiology

Xenopus laevis frogs were terminally anaesthetised by immersion in tricaine methanesulphonate (2 mg/ml, Sigma) in accordance with the Home Office Animals (Scientific Procedures) Act of 1986 or the Simon Fraser University Animal Care Committee and Canadian Council on Animal Care protocols and procedures. Stage V-VI oocytes were isolated and then defolliculated using a combination of collagenase treatment (1 h in 1 mg/ml collagenase type 1A; Sigma) and manual defolliculation. Defolliculated oocytes were incubated in Barth's medium at 19°C for 2-24 h before injection. Barth's medium contained (mM): 88 NaCl, 1 KCl, 2·4 $NaHCO_3$, 0·82 $MgSO_4$, 0·33 $Ca(NO_3)_2$, 0·41 $CaCl_2$, 20 Hepes, 1·25 sodium pyruvate, 0·1 mg/ml neomycin (Sigma) and 100 units/0·1 mg/ml penicillin/streptomycin mix (Sigma); titrated to pH 7·4 using NaOH. Oocytes were injected with 50 nl of cRNA encoding rat $K_v1.4$ (2·5 ng) or ferret $K_v1.4$ (5 ng) using a Drummond digital microdispenser (Broomall). In control experiments, oocytes were injected with 50 nl of DEPC-treated water; in these cases, currents were negligible compared to currents in cells injected with cRNA. After injection, oocytes were incubated in Barth's medium at 19°C for a further 16-48 h. During recording, oocytes were perfused with ND96 solution (mM: 96 NaCl, 3 KCl, 1 $MgCl_2$, 2 $CaCl_2$ and 5 Hepes; titrated to pH 7·4 using NaOH) at a flow rate of 0·5 ml/min. Experiments were performed at room temperature (20-22^{o}C). Currents were recorded using the two-electrode voltage clamp technique. Microelectrodes with a resistance of 0·6-3 MΩ (tip diameter, 1-5 μm) when filled with 3 M KCl were used. Membrane currents were recorded using a GeneClamp 500 amplifier (Axon Instruments) with computer-driven voltage protocols (Clampex software and Digidata 1200 interface, Axon Instruments). To construct current-voltage relationships for the wild-type $K_v1.4$ channel, currents were recorded during 200 ms pulses to potentials between -80 and +90 mV from a holding potential of -80 mV. The pulse frequency was 0.5 Hz (corresponding to a pulse interval of 2 s). To measure

recovery of the wild-type $K_v1.4$ channel from inactivation, a conditioning-test pulse protocol was used. Currents were recorded during a 200 ms test pulse to +40 mV at different test intervals following a 200 ms conditioning pulse to +40 mV (holding potential, -80 mV). The conditioning pulse frequency was 0·067 Hz (pulse interval, 15 s). In experiments on the mutant $K_v1.4$ △2-146 channel, currents were recorded during pulses of varying stated duration to +60 mV from a holding potential of -80 mV at a frequency of 0.017 Hz (pulse interval, 60 s). In all cases, quantification of inactivation was obtained as the degree of current decay at 4 s compared to the peak current. Conductance-voltage (G-V) relationships describing activation of $K_v1.4$ △2-146 and $K_v1.4$ △2-146 H508C mutant channels were determined from peak tail currents recorded during a –60 mV test voltage step that followed 90 ms depolarizing pulses ranging from -80 to +60 mV (in 10 mV increments) from a holding potential of -80 mV. Arachidonic acid (sodium salt; Sigma) was stored at -20°C as a 3 mM stock concentration in H_2O. EPA and DHA (Sigma) were stored at -20°C as a 3 mM stock concentration in 100% ethanol. The PUFAs were diluted in ND96 solution to obtain the desired concentration; the final concentration of ethanol was always <1%. Control experiments showed that 1% ethanol had no effect on $K_v1.4$. The PUFAs were diluted in ND96 solution immediately prior to an experiment; the PUFA-containing solution was made up fresh every 3 h and was protected from light to minimise oxidation of the PUFAs. In experiments in which the pH was varied, the ND96 solution was adjusted to the desired pH using NaOH. In experiments in which the K^+ concentration was raised, the KCl concentration of the ND96 solution was raised and the NaCl concentration was concomitantly reduced. The KCl and NaCl concentrations used were: 3 and 96 mM (normal), 50 and 49 mM, 100 and 0 mM, and 200 and 0 mM (note that the 200 mM K^+ solution was hypertonic). Oocytes were perfused with an altered solution for 10 min before recording. Data analysis was performed

using pCLAMP software (Axon Instruments), SigmaPlot (SPSS Science) and SigmaStat (Jandel Scientific Software). Data are shown as means ± SEM (number of oocytes).

Structural modelling

A comparative model had been constructed previously (31) for the pore domain (S5-S6) of $K_v1.4$ based on the crystal structure for the equivalent part of rat $K_v1.2$ (Protein Data Bank id 2a79) (32). The pore domain was placed at the centre of a cylindrical slab of low dielectric atoms, representing the membrane. Binding of arachidonic acid was modelled using the program Swiss-PdbViewer (18), with the hydrophobic chain lying approximately along the transmembrane axis, and presented to the non-polar exterior of the pore domain, without overlapping the additional domains (S1-S4) present in the voltage-gated K^+ channels (32). The acidic head group was protruding from the modelled membrane.

In order to assess the relative charge interactions between the arachidonic acid head group, a K^+ ion at the entrance to the selectivity filter and H508, a dipole was balanced between the histidine residue and the S_1 binding site for K^+ in the selectivity filter. The pattern of potential from this dipole effectively shows the division of neighbouring regions into those which interact more strongly with either of these two sites. The charge for these calculations was -1e on H508 and +1e at the selectivity filter, setting up the dipole rather than reflecting physiological charge. Dipole potential was computed using the Finite Difference Poisson-Boltzmann method (49), with relative dielectrics of 4 for protein and membrane and 78.4 for solvent, at an ionic strength of 0.15 M.

Results

PUFAs inhibit $K_v1.4$ by slowing recovery from inactivation

Wild-type $K_v1.4$ current was recorded during 200 ms pulses from a holding potential of -80 mV to potentials up to +90 mV at a pulse frequency of 0·5 Hz. Fig. 1 shows that wild-

type $K_v1.4$ current was inhibited by 50 μM arachidonic acid, 15 μM EPA and 50 μM DHA during repetitive pulsing. Fig. 1A shows the effect of arachidonic acid, EPA and DHA on current at +90 mV and Fig. 1B shows the effect on the current-voltage relationship. The PUFAs reduced wild-type $K_v1.4$ current at most potentials (Fig. 1B). Extracellular acidosis has a similar action on wild-type $K_v1.4$ current during repetitive pulsing and it is the result of a slowing of recovery from inactivation (12). A conditioning-test pulse protocol was used to measure the recovery of wild-type $K_v1.4$ from inactivation at -80 mV. Fig. 2A shows superimposed currents at different test intervals (between the conditioning and test pulses) under control conditions and in the presence of 50 μM arachidonic acid, DHA or 15 μM EPA. Fig. 2B shows the time course of recovery from inactivation. $K_v1.4$ current during the test pulse (measured as the difference between peak current and the current at the end of the pulse) is expressed as a percentage of the current during the conditioning pulse and plotted against the test interval. Fig. 2B shows that recovery from inactivation was slowed by arachidonic acid, EPA and DHA. The recovery was fitted by a double exponential function; the slower time constant was increased to 7.2±1.6 s in the presence of 50 μM arachidonic acid (from 2.1±0.1 s under control conditions; paired t-test, $P<0.01$) and 3.5±0.4 s in the presence of 50 μM DHA (from 1.8±0.2 s under control conditions; paired t-test, $P<0.01$). Recovery from inactivation in the presence of 15 μM EPA showed a similar trend, the time course was 4.11±1.4 s in the presence of EPA and 2.4±0.9 s under control conditions, but this did not reach statistical significance. Inspection of Fig. 2B suggests that the slowing of recovery from inactivation can explain the inhibition of wild-type $K_v1.4$ current during repetitive pulsing at a frequency of 0.5 Hz (pulse interval, 2 s; Fig. 1). Indeed this is demonstrated in Fig. 2C and D, which show that wild-type $K_v1.4$ current is no longer reduced by 50 μM arachidonic acid when repetitive pulsing was slowed to a frequency of 0.017 Hz to allow for complete recovery of channels from N-type inactivation between voltage steps.

Effect of PUFAs on C-type inactivation

Although inactivation of wild-type $K_v1.4$ channels is dominated by rapid entry into the N-type inactivated state, recovery from inactivation is determined by the recovery from C-type inactivation (41). Therefore, it is possible that the PUFAs affect C-type inactivation. The effect of PUFAs on C-type inactivation was investigated using a deletion mutant, $K_v1.4$ △2-146, which lacks N-type inactivation (41). $K_v1.4$ △2-146 current was recorded during 7.5 s pulses to +60 mV (pulse frequency, 0.017 Hz) from a holding potential of -80 mV. During the pulse, C-type inactivation was observed – it was slower than N-type inactivation (compare Figs. 1 and 3). Fig. 3A shows $K_v1.4$ △2-146 current recorded under control conditions and during the application of arachidonic acid. At this slow rate of pulsing, the application of arachidonic acid did not reduce peak current, but accelerated the rate of entry of channels into the C-type inactivated state. The effect of arachidonic acid appeared to occur maximally upon the first voltage pulse in the presence of the PUFA and did not alter with prolonged exposure. These data are consistent with those collected in N-type inactivating wild-type channels suggesting that arachidonic acid does not block the channel, but rather stabilises the C-type inactivated state. This is further supported by the data shown in Fig. 3B and C, which demonstrate the effects of arachidonic acid on $K_v1.4$ △2-146 current decay during voltage pulses of duration that varied from 7.5 to 30 s. These data show that current decay approximates a steady-state value by the end of a 30 s long pulse to +60 mV that represents the equilibrium between open and inactivated states. Arachidonic acid reduced the current level indicative of an induced stabilisation of the C-type inactivated state. This bias towards the C-type inactivated state could be measured with similar accuracy at numerous time-points throughout the current decay (Fig. 3C), and therefore, in order to simplify data acquisition and analysis, all future quantification of inactivation is presented as the percentage current decay at 4 s.

Fig. 3D and E show the effect of different concentrations of arachidonic acid, EPA or DHA on C-type inactivation in $K_v1.4$ △2-146 channels. Arachidonic acid, EPA and DHA stabilised the C-type inactivated state in a concentration-dependent manner. This is highlighted by the dose-response curves in Fig. 3E in which the percentage inactivation at 4 s is plotted against the concentration of the PUFAs. The K_D for the effect of arachidonic acid, EPA and DHA on C-type inactivation was 43, 15 and 18 μM, respectively.

Interaction among the effects of extracellular PUFAs, H^+ and K^+ on $K_v1.4$

C-type inactivation of $K_v1.4$ is also known to be affected by extracellular H^+ and K^+ (12); (28); (13). Fig. 4A shows $K_v1.4$ △2-146 current in different extracellular K^+ concentrations (from 3 to 200 mM) and at different extracellular pH values (from 6.5 to 8.5). At each extracellular K^+ concentration, decreasing the pH value can be seen to stabilise the C-type inactivated state. On the other hand, raising the extracellular K^+ concentration can be seen to destabilise the C-type inactivated state. Furthermore, Fig. 4A shows that there was an interaction between the effects of extracellular K^+ and extracellular pH, because the effect of extracellular pH was less at higher extracellular K^+ concentrations – conversely, the effect of extracellular K^+ was greater at lower pH values. This is confirmed by the titration curves in Fig. 4B – the percentage inactivation at 4 s is plotted against the concentration of extracellular H^+. The titration curve for $K_v1.4$ △2-146 is shifted to the right at higher extracellular K^+ concentrations. In Fig. 4C, the pK_a (the pH value at which the pH effect is half maximal) is plotted against the extracellular K^+ concentration. The pK_a decreased as the extracellular K^+ concentration was raised reflecting a ~30-fold increase in the K_D of proton binding in response to increasing external K^+ from 3 to 200 mM.

The effect of a decrease in extracellular pH or extracellular K^+ on C-type inactivation is similar to the action of PUFAs (compare Figs. 3 and 4). Therefore, is there an interaction among the effects of extracellular PUFAs, H^+ and K^+ on C-type inactivation? Fig. 5A shows

the effect of 30 μM arachidonic acid, EPA and DHA on $K_v1.4$ △2-146 current at pH 7.4 and 5.5 or 6.0. In each case, the presence of the PUFA reduced the effect of acidic pH on C-type inactivation. In Fig. 5B, titration curves for $K_v1.4$ △2-146 are shown in the absence and presence of 30 μM arachidonic acid. They show that, in the presence of arachidonic acid, the titration curve was flattened, i.e. the pH dependence of the channel was markedly reduced. The titration curves in Fig. 5B also suggest that arachidonic acid caused a *destabilisation* of the C-type inactivated state at acidic pH. Although titration curves in the presence of EPA and DHA are not shown, mean data in Fig. 5B confirm that EPA and DHA also destabilised the C-type inactivated state at pH 6.0.

Fig. 6A shows the effect of 30 μM arachidonic acid, EPA and DHA on $K_v1.4$ △2-146 current in 3 and 100 mM extracellular K^+. Whereas in 3 mM extracellular K^+ the PUFAs enhanced C-type inactivation, in 100 mM K^+ they had little effect (Fig. 6A). This is confirmed by Fig. 6B, which shows the percentage inactivation at 4 s in the absence and presence of the PUFAs in 3 and 100 mM extracellular K^+. The results shown in Figs. 5 and 6 demonstrate that there is an interaction among the effects of extracellular PUFAs, H^+ and K^+ on C-type inactivation.

Involvement of two positively-charged pore residues (H508 and K532)

We have previously shown that H508 and K532 mediate the acidosis-induced enhancement of C-type inactivation of $K_v1.4$ (13). Because there is an interaction among the effects of extracellular PUFAs, H^+ and K^+ on C-type inactivation, all three may have a common site of action. We, therefore, investigated the effect of PUFAs on $K_v1.4$ △2-146 in which H508 or K532 was substituted by a cysteine residue. Fig. 7 shows the effect of 30 μM arachidonic acid, EPA and DHA on the mutated forms of $K_v1.4$ △2-146 (typical currents and mean percentage inactivation at 4 s are shown). The current profile of the $K_v1.4$ △2-146 H508C and $K_v1.4$ △2-146 K532C mutant channels was the same as that of the $K_v1.4$ △2-

146 channel. However, whereas 30 μM arachidonic acid, EPA and DHA had a marked effect on C-type inactivation of K_v1.4 △2-146 (e.g. Fig. 3), 30 μM arachidonic acid, EPA and DHA had no effect on both K_v1.4 △2-146 H508C and K_v1.4 △2-146 K532C (Fig. 7). Higher concentrations of arachidonic acid (70 μM) failed to induce a notable change in the rate of or steady-state C-type inactivation in K_v1.4 △2-146 H508C channels (data not shown), suggesting that the effect of PUFAs on C-type inactivation is abolished with the mutations.

Two separable mechanisms of action of arachidonic acid

Interestingly, although the H508C mutation abolished the effect of arachidonic acid on C-type inactivation, the mutation had no impact on the effect of arachidonic acid on the voltage-dependence of activation. Fig. 8A shows that arachidonic acid induces a hyperpolarizing shift in the voltage-dependence of K_v1.4 △2-146 activation in a manner that is similar to that described previously for the action of PUFAs in *Shaker*, K_v1.2, K_v1.5, K_v2.1, K_v7.1 and K_v11.1 channels (7; 20; 30; 34; 40). K_v1.4 △2-146 currents recorded in response to 90 ms step depolarizations applied from -80 to +60 mV are shown along with relative conductance-voltage relationships plotted from peak tail currents recorded at -60 mV and fitted using the Boltzmann equation. Application of arachidonic acid induced an -8.8 ± 1.5 mV (n=11) shift in the $V_{1/2}$ of activation. Such modulation of the voltage-dependence of K_v channel activation by PUFAs has been best characterised in *Shaker* channels and has been described as a lipoelectric effect due to an electrostatic interaction of PUFAs with an extracellular voltage sensor site (7). Further examination of the effects of arachidonic acid on K_v1.4 △2-146 H508C mutant channels (Fig. 8B) reveals that the lipoelectric effect of arachidonic acid is preserved in H508C channels despite the abolition of the effect on C-type inactivation. In K_v1.4 △2-146 H508C channels, arachidonic acid induced an -11.6 ± 1.0 mV shift (n=5; t-test $P>0.1$ when compared to the shift induced in K_v1.4 △2-146 channels) in the

$V_{1/2}$ of activation. These data suggest two effects of arachidonic acid in $K_v1.4$ channels that are separable by selective abolition of the effects on C-type inactivation by the H508C outer pore mutation, which does not alter the PUFA-induced lipoelectric effect.

Structural modelling

Fig. 9A shows a section through the modelled $K_v1.4$ pore domain (S5-S6) used in our charge calculations – only two of the four subunits are shown for clarity and the positions of H508 and K532 are shown. This was brought together with an arachidonic acid molecule in a cylindrical membrane slab. Arachidonic acid (shown on the left hand side of Fig. 9A), like other PUFAs, consists of a hydrophobic tail and a negatively-charged (i.e. acidic) head group (shown in red on the left hand side of Fig. 9A). Arachidonic acid is modelled in the membrane with the negatively-charged head group protruding (Fig. 9B). The calculated dipolar potential from H508 (shown in red in Fig. 9B) and a K^+ site at the selectivity filter (shown in blue in Fig. 9B; see Methods) suggests that arachidonic acid could interact more strongly with the charge at H508 than with the charge at the selectivity filter. This suggests only a relatively small direct interaction between the negatively-charged arachidonic acid head group and a K^+ ion in the selectivity filter. Fig. 9B suggests instead that there is an indirect interaction: the negative charge of the arachidonic acid head group is expected to stabilise the protonated form of H508 (i.e. raise its pK_a), which in turn is expected to destabilise K^+ ions in the selectivity filter, leading to the observed stabilisation of the C-type inactivated state. In the absence of H508, there would be a lesser effect or no effect of PUFAs, as observed in Fig. 7A.

Discussion

This study has shown that K^+ current flow through the $K_v1.4$ channel is inhibited by PUFAs during repetitive pulsing and that this is the result of a slowing of recovery of $K_v1.4$

from inactivation, which in turn arises from a stabilisation of channels in the C-type inactivated state. The effect of PUFAs is similar to that of extracellular acidosis or a decrease of extracellular K^+ and indeed there is an interaction among the three effects. The effect of PUFAs can be abolished by mutation of two positively-charged residues in the extracellular pore region of the channel, as can the effects of extracellular H^+ and K^+. A model has been put forward to explain the action of PUFAs at the molecular level, which suggests that the mechanism by which PUFAs act on C-type inactivation is mediated by outer pore residues and is distinct from the lipoelectric effect of PUFAs on the voltage-dependence of K_v channel activation that is mediated via interactions with the voltage sensor.

Mechanism of action of PUFAs on C-type inactivation

Although in no other study has the site of action of PUFAs on C-type inactivation been addressed, inactivation in K_v4 (22); (43) and $K_v1.5$ channels (23) has been reported to be enhanced by arachidonic acid and DHA. Oliver et al. also (39) showed that arachidonic acid enhanced inactivation in $K_v3.1$ channels and went on to show that the effects are not mediated via intracellular pore block, but rather conformational changes at the selectivity filter. However, in none of these studies was evidence provided for a site and mechanism of action of PUFAs on inactivation.

The data in Figure 2C and 3A suggest that PUFAs act at an extracellular site outside of the permeation pathway to modify C-type inactivation in $K_v1.4$ and $K_v1.4$ Δ2-146 channels. A pore block mechanism is inconsistent with the observation that peak $K_v1.4$ current is not inhibited by arachidonic acid when the pulse frequency is slowed to allow for complete recovery from inactivation (Fig. 2C). Furthermore, in $K_v1.4$ Δ2-146 channels, the maximal effect of a given concentration of arachidonic acid can be observed in the first recording following application of the PUFA (Fig. 3A), suggesting an extracellular site of action and no accumulation of channel block. This is also consistent with the observation that

mutation of the outer pore residues, H508 and K532, abolishes the effects of arachidonic acid on C-type inactivation (Fig. 7). Such side-specificity of PUFA interaction has been reported previously in other K_v channels. DHA inhibits K_v1.2 channels extracellularly (40), and linoleic acid modulates K_v2.1 from the extracellular side (34). Similarly, the inhibitory effects of α-linolenic acid, arachidonic acid, DHA, and linoleic acid on K_v1.5 channels are externally mediated (21; 23; 34). In contrast, the arachidonic acid derivative, anandamide, inhibits K_v1.5 channels via an intracellular pore block mechanism (36). A non-specific action of PUFAs on K_v1.4 (for example, a detergent effect and a change in membrane fluidity) is unlikely, because the PUFA-induced inactivation of the channel was reversed by extracellular acidosis (Fig. 5), abolished by raised extracellular K^+ (Fig. 6) and abolished by the mutation of two positively-charged extracellular pore residues, H508 and K532 (Fig. 7). An outer pore PUFA interaction site that modulates C-type inactivation in K_v1.4 channels is therefore a novel finding that is consistent with previous observations of the effects of PUFAs in other channels.

Separable mechanisms of PUFA-induced modulation of K_v1.4 channel function

There is evidence that PUFAs interact with K_v channels via multiple sites/mechanisms. For example, in addition to inhibiting current, PUFAs have been shown to shift the voltage-dependence of activation to more negative potentials in *Shaker* (7), K_v1.2 (40), K_v1.5 and K_v2.1 (34), K_v7.1 (30) and K_v11.1 (20) channels. Data shown in Fig. 8 demonstrate a similar phenomenon in K_v1.4 channels. Interestingly, the H508C mutation abolished the effects of arachidonic acid on C-type inactivation without modifying the effect on the voltage-dependence of activation. Börjesson et al., (6; 7) characterised the modification of activation voltage-dependence by *cis* *ω*-3 and *ω*-6 fatty acids in *Shaker* channels as a lipoelectric mechanism, where charged PUFAs electrostatically interact with the voltage-sensor during its final outward transition leading to the channel opening.

Recently, Liin et al. (30) also demonstrated a similar PUFA modulation and binding site on $K_v7.1$ channels. The data in the present study are the first, to our knowledge, to demonstrate that the lipoelectric effect is observed in $K_v1.4$ channels, and therefore we chose to focus on the separation of this effect from that on inactivation using a test candidate, arachidonic acid. The similarity in the lipoelectric effect of a range of PUFAs in the above mentioned channels would suggest that we would see a similar result in $K_v1.4$ channels with DHA and EPA. The separation of effects of arachidonic acid in $K_v1.4$ channels by the H508C mutation suggests that there are two extracellular arachidonic acid interaction sites, one on the voltage sensor, which mediates the lipoelectric effect, and one in the outer mouth of the pore, which mediates the effect on C-type inactivation. Alternatively, a common interaction site may elicit two separable effects, one of which, that on C-type inactivation, can be disrupted by the H508C mutation. The modelling data shown in Fig. 9, which suggest that arachidonic acid interacts directly with H508 to alter its charge and therefore pore occupancy of K^+ and consequently C-type inactivation (see below), favours the former possibility. Interestingly, a previous study describing the effect of linoleic acid on $K_v1.5$ and $K_v2.1$ channels also concluded that there are two distinct mechanisms that allow the PUFA to affect both activation and inactivation, although the exact mechanisms were not established (34).

Interaction among the effects of extracellular PUFAs, H^+ and K^+ and the role of pore charges

The effect of PUFAs on C-type inactivation of $K_v1.4$ was similar to the actions of extracellular H^+ and K^+ (Figs. 3 and 4). There was an interaction between the effects of extracellular H^+ and K^+ on the $K_v1.4$ channel: acidosis acted to increase C-type inactivation and this effect was reduced on moving from 3 to 200 mM K^+, which by itself acted to decrease C-type inactivation (Fig. 4). There was also an interaction among the effects of extracellular PUFAs, H^+ and K^+: extracellular acidosis reversed the PUFA-induced

enhancement of C-type inactivation of $K_v1.4$, while raised extracellular K^+ abolished it (Figs. 5 and 6). An interaction between extracellular H^+ and K^+ in mediating C-type inactivation is consistent with a previous study from our laboratory on the wild-type $K_v1.4$ channel (14); see also Li et al. (28), as well as studies in $K_v1.3$ (45), $K_v1.4$ (12); (13), and $K_v1.5$ (16) channels, which identify outer pore residues, e.g. H508 and K532 in $K_v1.4$, as pH sensor sites. It is well established that raising extracellular K^+ abolishes C-type inactivation by occupying the pore and preventing pore collapse, while acidosis enhances C-type inactivation (via interaction with H508) decreasing K^+ occupancy of the pore and thus enhancing C-type inactivation (1; 13; 31; 41). We, and others, have also shown that raising extracellular K^+ abolishes the effect of acidosis by preventing the pore collapse due to inactivation (13; 31). Here, we propose that PUFAs act, like acidosis, via H508. This conclusion is consistent with the PUFA-induced stabilisation of C-type inactivation (Fig. 3) as well as the observation that extracellular K^+ abolishes the effect of PUFAs (Fig. 4). Figure 5 shows that there is an interaction between the action of PUFAs and H+, where the effect of PUFAs was reduced in the presence of protons. Borjesson *et al*., (7) observed a similar pH-dependence to the effect of PUFAs on the lipoelectric effect in *Shaker* channels. They reasoned that protonation of the PUFA headgroup reduced the effect of the PUFA suggesting an electrostatic mechanism. We propose that protonation of membrane embedded PUFAs at low pH alters the PUFA interaction with the H508 charge in a similar way, preventing it from stabilising the inactivated configuration. Depending on the pH, not all PUFAs will be protonated and some H508 sites may be free to interact with protons producing a net effect of a partial relief of the PUFA-induced stabilisation of inactivation at acidic pH (Fig. 5).

The data in Fig. 7 show that mutation of H508 or K532 extracellular charges abolished the PUFA-induced enhancement of C-type inactivation. The effect of mutation of H508 was specific in its abolition of the action of PUFAs on inactivation, without modifying

the effect of PUFAs on activation gating, provides strong evidence for a role of this sites in mediating the effects of PUFAs on K_v1.4 inactivation. Modelling studies (Fig. 9) suggest that increasing the positive charge at H508 stabilises C-type inactivation by increasing repulsive interactions with K^+ ions. We propose that mutation of K532 alters inactivation. In previous work, we showed that K532 is an important site for inactivation in Kv1.4 channels, not as a titratable site, but rather as a site that tunes the electrostatic profile of the pore that a K^+ ion encounters (14; 31). Continuum electrostatic modelling suggested that mutations at K532 alter the electrostatic profile such that K^+ occupancy is favoured regardless of charge modification at H508 (31). The data in the present study are consistent with this in that mutation of K532 abolishes the effects of PUFAs on C-type inactivation. These data suggest that mutation of K532 increases K^+ occupancy to such an extent that PUFA modification of H508 charge does not reduce K^+ occupancy sufficiently to stabilise C-type inactivation. Our interpretation of these collected data is that H508 is the proton-sensor, and also the PUFA-sensitive residue with protons and PUFAs acting via a common mechanism that involves K532, which is known to be linked to C-type inactivation in K_v1.4 and other channels (12); (33).

A possible common mechanism of action of PUFAs

Modelling the effects of extracellular protons on K^+ coordination within the K_v1.4 outer pore has suggested that the increased positive charge of the protonated H508 residue electrostatically reduces K^+ occupancy of the selectivity filter, thus promoting C-type inactivation (31). K^+ occupancy of the selectivity filter is thought to control the constriction of the selectivity filter during C-type inactivation (38), which is dictated by the exit of K^+ from the pore (2) . As shown in Fig. 9, it is proposed that the hydrophobic tail of PUFAs lies within the membrane and that the negatively-charged head group interacts with H508. The effect of this will be to favour protonation of H508 (i.e. to increase the pK_a of H508) and,

therefore, ultimately C-type inactivation. The experimental data suggest that a PUFA at its K_D must increase the pK_a for C-type inactivation from 6.7 (normal value at an extracellular K^+ concentration of 3 mM; Fig. 4) to 7.4 (because C-type inactivation is half-maximally increased at pH 7.4 in the presence of a PUFA at its K_D; Fig. 5B). Calculations of the effect of binding one arachidonic acid molecule per monomer unit of the 2a79 crystal structure, i.e. four arachidonic acid molecules in total, as described in the Methods section, gives an estimate of a pK_a shift of ~0.4 for each H508 sidechain. This estimate would be affected by conformational change and the location of arachidonic acid binding to transmembrane regions of the pore domain exterior. Nevertheless, in comparison with the experimentally observed pK_a change of 0.7 it may indicate, within the confines of our model, that more than one arachidonic acid molecule binds per channel monomer. This hypothesis is consistent with the study of Smirnov and Aaronson (44), who found that a neutral fatty acid has a smaller inhibitory effect on delayed rectifier K^+ current in rat pulmonary arterial myocytes than a negatively-charged one.

The modelling data in Fig. 9 could explain why extracellular PUFAs, H^+ and K^+ had similar effects and why there was an interaction among them and why mutation of H508 abolishes the effects. We propose that the positively-charged K532 residue electrostatically affects the K^+ occupancy of the selectivity filter – it tonically reduces the K^+ occupancy to a point at which C-type inactivation is sensitive to further changes in K^+ occupancy (31). This explains the effect of neutralisation of K532: after its replacement there is an increase in K^+ occupancy and the PUFA-facilitated protonation of H508 no longer decreases K^+ occupancy sufficiently to trigger C-type inactivation. One finding that remains to be explained is why acidosis reverses the effect of PUFAs (Fig. 5). We suggest that at low pH, PUFAs no longer affect the channel via an *indirect effect* on the pK_a of H508, but instead, via a weak *direct effect* (normally masked by the stronger indirect effect): the negatively-charged head group of

PUFAs may *negate* some of the positive charge of H508 (which by itself tends to reduce the K^+ occupancy of the selectivity filter and favour C-type inactivation).

Our data suggest that arachidonic acid stabilizes C-type inactivation by modifying the electrostatic potential at the outer mouth of the pore, which reduces K^+ occupancy. Although the rate and extent of C-type inactivation varies greatly between K_v channels, even those within the same sub-family, we speculate that PUFA modification of the potential profile of the outer pore may be a general mechanism by which PUFAs modulate C-type inactivation in K_v channels. Our data would suggest that channels with an equivalent His residue to H508, such as $K_v1.5$, would also demonstrate PUFA-dependent stabilisation of C-type inactivation via charge modification of the His as reported here for $K_v1.4$ channels. Indeed, pH-dependence of C-type inactivation has been shown in $K_v1.5$ to be mediated by an equivalent His pore residue (46). However, the site of action of PUFAs is likely different in different channels, since this His is not highly conserved. For example, it is absent in $K_v1.2$ channels, which display PUFA-dependent inactivation. Furthermore, other PUFA-sensitive channels, such as $K_v2.1$ and $K_v3.1$, undergo a complex inactivation process that involves C-type inactivation, but also pronounced U-type inactivation that has been characterised as inactivation from closed states (25; 26). Our findings of the site of action may not extrapolate to such cases, but we propose that PUFA-induced modification of K^+ occupancy may be a general mechanism of action.

The physiological relevance of modulation of $K_v1.4$ by PUFAs

Besides the effects of PUFAs on cloned channels, PUFAs have also been shown to affect native outward rectifier K^+ currents: for example, in hippocampal neurones and retinal cells, arachidonic acid enhances inactivation and reduces the amplitude of transient outward K^+ current (24); (9). In the heart, the transient outward K^+ current is generated by $K_v1.4$,

$K_v4.2$ and $K_v4.3$ channels and EPA and DHA enhance inactivation and reduce the amplitude of the transient outward K^+ current in rat and ferret cardiac myocytes (5); (50).

Arachidonic acid, EPA and DHA increased C-type inactivation of $K_v1.4$ with a K_D of 43, 15 and 18 μM, respectively (Fig. 3). This suggests that $K_v1.4$ can be modulated by the PUFAs under physiological and pathophysiological conditions – the plasma concentration of ω-3 PUFAs in the human can be up to 200-400 μM (see Introduction). In the heart, because $K_v1.4$ is one of the channels responsible for I_{to}, an important determinant of the cardiac action potential duration, modulation of $K_v1.4$ by ω-6 and ω-3 PUFAs may affect the dispersion of repolarization and the propensity for ventricular arrhythmias during myocardial ischaemia when the concentration of arachidonic acid is raised (11). However, modulation of $K_v1.4$ by PUFAs is unlikely to be the only mechanism responsible for any beneficial action of PUFAs on the heart, because the PUFAs affect other targets. If modulation of $K_v1.4$ by PUFAs is important, as shown in Figs. 5 and 6, the effect of PUFAs is expected to be affected by extracellular pH and K^+. Accumulation of PUFAs, acidosis and raised extracellular K^+ occur in many pathological conditions. For example, in the heart, during metabolic inhibition, extracellular pH can decrease to 6, extracellular K^+ can increase to 12 mM and PUFAs can be released as a result of phospholipase A_2 activity. The PUFAs, acidosis and raised extracellular K^+ will each affect $K_v1.4$, but there will also be an interaction among the effects. The consequences of such pathological conditions are, therefore, complex.

Acknowledgements

This work was supported by a Heart and Stroke Foundation of B.C. and Yukon Grant-in-Aid (G-15-0009086; TWC) and a Natural Sciences and Engineering Council (RGPIN-04759 NSERC) of Canada Discovery Grant (TWC). DJ holds a NSERC Canada Graduate Scholarship.

Reference List

1. **Baukrowitz T and Yellen G. Modulation of K^+ current by frequency and external [K^+]: a tale of two inactivation mechanisms. *Neuron* 15: 951-960, 1995.**

2. **Baukrowitz T and Yellen G. Use-dependent blockers and exit rate of the last ion from the multi-ion pore of a K^+ channel. *Science* 271: 653-656, 1996.**

3. **Bhatnagar A. Beating ischemia: a new feat of EETs? *Circ Res* 95: 443-445, 2004.**

4. **Billman GE, Hallaq H and Leaf A. Prevention of ischemia-induced ventricular fibrillation by omega 3 fatty acids. *Proc Natl Acad Sci U S A* 91: 4427-4430, 1994.**

5. **Bogdanov KY, Spurgeon HA, Vinogradova TM and Lakatta EG. Modulation of the transient outward current in adult rat ventricular myocytes by polyunsaturated fatty acids. *Am J Physiol* 274: H571-H579, 1998.**

6. **Borjesson SI and Elinder F. An electrostatic potassium channel opener targeting the final voltage sensor transition. *J Gen Physiol* 137: 563-577, 2011.**

7. **Borjesson SI, Hammarstrom S and Elinder F. Lipoelectric modification of ion channel voltage gating by polyunsaturated fatty acids. *Biophys J* 95: 2242-2253, 2008.**

8. **Brahmajothi MV, Campbell DL, Rasmusson RL, Morales MJ, Trimmer JS, Nerbonne JM and Strauss HC. Distinct transient outward potassium current (ito) phenotypes and distribution of fast-inactivating potassium channel alpha subunits in ferret left ventricular myocytes. *J G P* 113: 581-600, 1999.**

9. **Bringmann A, Skatchkov SN, Biedermann B, Faude F and Reichenbach A. Alterations of potassium channel activity in retinal Muller glial cells induced by arachidonic acid. *Neuroscience* 86: 1291-1306, 1998.**

10. **Calon F, Lim GP, Morihara T, Yang F, Ubeda O, Salem N, Jr., Frautschy SA and Cole GM. Dietary n-3 polyunsaturated fatty acid depletion activates caspases and decreases NMDA receptors in the brain of a transgenic mouse model of Alzheimer's disease. *Eur J Neurosci* 22: 617-626, 2005.**

11. **Chien KR, Han A, Sen A, Buja LM and Willerson JT. Accumulation of unesterified arachidonic acid in ischemic canine myocardium. Relationship to a phosphatidylcholine deacylation-reacylation cycle and the depletion of membrane phospholipids. *Circ Res* 54: 313-322, 1984.**

12. **Claydon TW, Boyett MR, Sivaprasadarao A, Ishii K, Owen JM, O'Beirne HA, Leach R, Komukai K and Orchard CH. Inhibition of the K^+ channel Kv1.4 by acidosis: protonation of an extracellular histidine slows the recovery from N-type inactivation. *J Physiol* 526: 253-264, 2000.**

13. **Claydon TW, Boyett MR, Sivaprasadarao A and Orchard CH. Two pore residues mediate acidosis-induced enhancement of C-type inactivation of the Kv1.4 K^+ channel. *Am J Physiol* 283: C1114-C1121, 2002.**

14. **Claydon TW, Makary SY, Dibb KM and Boyett MR. K+ activation of kir3.1/kir3.4 and kv1.4 K+ channels is regulated by extracellular charges. *Biophys J* 87: 2407-2418, 2004.**

15. **Das UN and Fams. Long-chain polyunsaturated fatty acids in the growth and development of the brain and memory. *Nutrition* 19: 62-65, 2003.**

16. **Fedida D, Zhang S, Kwan DC, Eduljee C and Kehl SJ. Synergistic inhibition of the maximum conductance of Kv1.5 channels by extracellular K+ reduction and acidification. *Cell Biochem Biophys* 43: 231-242, 2005.**

17. **Gubitosi-Klug RA, Yu SP, Choi DW and Gross RW. Concomitant acceleration of the activation and inactivation kinetics of the human delayed rectifier K+ channel (Kv1.1) by Ca(2+)-independent phospholipase A2. *J Biol Chem* 270: 2885-2888, 1995.**

18. **Guex N and Peitsch MC. Swiss-model and the Swiss-PdbViewer: An environment for comparative protein modeling. *Electrophoresis* 18: 2714-2723, 1997.**

19. **Guizy M, Arias C, David M, Gonzalez T and Valenzuela C. {Omega}-3 and {omega}-6 polyunsaturated fatty acids block HERG channels. *Am J Physiol Cell Physiol* 289: C1251-C1260, 2005.**

20. **Guizy M, Arias C, David M, Gonzalez T and Valenzuela C. {Omega}-3 and {omega}-6 polyunsaturated fatty acids block HERG channels. *Am J Physiol Cell Physiol* 289: C1251-C1260, 2005.**

21. **Guizy M, David M, Arias C, Zhang L, Cofan M, Ruiz-Gutierrez V, Ros E, Lillo MP, Martens JR and Valenzuela C. Modulation of the atrial specific Kv1.5 channel by the n-3 polyunsaturated fatty acid, alpha-linolenic acid. *J Mol Cell Cardiol* 44: 323-335, 2008.**

22. **Holmqvist MH, Cao J, Knoppers MH, Jurman ME, Distefano PS, Rhodes KJ, Xie Y and An WF. Kinetic modulation of Kv4-mediated A-current by arachidonic acid is dependent on potassium channel interacting proteins.** ***J Neurosci*** **21: 4154-4161, 2001.**

23. **Honore E, Barhanin J, Attali B, Lesage F and Lazdunski M. External blockade of the major cardiac delayed-rectifier K+ channel (Kv1.5) by polyunsaturated fatty acids.** ***Proc Natl Acad Sci U S A*** **91: 1937-1941, 1994.**

24. **Keros S and McBain CJ. Arachidonic acid inhibits transient potassium currents and broadens action potentials during electrographic seizures in hippocampal pyramidal and inhibitory interneurons.** ***J Neurosci*** **17: 3476-3487, 1997.**

25. **Klemic KG, Kirsch GE and Jones SW. U-type inactivation of Kv3.1 and** ***Shaker*** **potassium channels.** ***Biophys J*** **81: 814-826, 2001.**

26. **Klemic KG, Shieh CC, Kirsch GE and Jones SW. Inactivation of Kv2.1 potassium channels.** ***Biophys J*** **74: 1779-1789, 1998.**

27. **Kris-Etherton PM, Harris WS and Appel LJ. Fish consumption, fish oil, omega-3 fatty acids, and cardiovascular disease.** ***Circulation*** **106: 2747-2757, 2002.**

28. **Li X, Bett GC, Jiang X, Bondarenko VE, Morales MJ and Rasmusson RL. Regulation of N- and C-type inactivation of Kv1.4 by pHo and K^+: evidence for transmembrane communication.** ***Am J Physiol Heart Circ Physiol*** **284: H71-H80, 2003.**

29. **Liin, S. I., Larsson, J. E., Barro-Soria, R., Skarsfeldt, M. A., Bentzen, B. H., and Larsson, H. P. Arachidonoyl Taurine Rescues Diverse Long QT Syndrome-**

Associated Mutations in the Cardiac IKs Channel. Biophysical Journal 110, 185a-186a. 2016.

30. Liin SI, Silvera EM, Barro-Soria R, Skarsfeldt MA, Larsson JE, Starck HF, Parkkari T, Bentzen BH, Schmitt N, Larsson HP and Elinder F. Polyunsaturated fatty acid analogs act antiarrhythmically on the cardiac IKs channel. *Proc Natl Acad Sci U S A* 112: 5714-5719, 2015.

31. Liu B, Westhead DR, Boyett MR and Warwicker J. Modelling the pH-dependent properties of Kv1 potassium channels. *J Mol Biol* 368: 328-335, 2007.

32. Long SB, Campbell EB and MacKinnon R. Crystal structure of a mammalian voltage-dependent *Shaker* family K^+ channel. *Science* 309: 897-903, 2005.

33. Lopez-Barneo J, Hoshi T, Heinemann SH and Aldrich RW. Effects of external cations and mutations in the pore region on C-type inactivation of *Shaker* potassium channels. *Receptors and Channels* 1: 61-71, 1993.

34. McKay MC and Worley JF, III. Linoleic acid both enhances activation and blocks Kv1.5 and Kv2.1 channels by two separate mechanisms. *Am J Physiol Cell Physiol* 281: C1277-C1284, 2001.

35. Meves H. Modulation of ion channels by arachidonic acid. *Prog Neurobiol* 43: 175-186, 1994.

36. Moreno-Galindo EG, Barrio-Echavarria GF, Vasquez JC, Decher N, Sachse FB, Tristani-Firouzi M, Sanchez-Chapula JA and Navarro-Polanco RA. Molecular basis for a high-potency open-channel block of Kv1.5 channel by the endocannabinoid anandamide. *Mol Pharmacol* 77: 751-758, 2010.

37. **Nelson TJ, Collin C and Alkon DL. Isolation of a G protein that is modified by learning and reduces potassium currents in Hermissenda. *Science* 247: 1479-1483, 1990.**

38. **Ogielska EM and Aldrich RW. Functional consequences of a decreased potassium affinity in a potassium pore. Ion interactions and C-type inactivation. *J Gen Physiol* 113: 347-358, 1999.**

39. **Oliver D, Lien CC, Soom M, Baukrowitz T, Jonas P and Fakler B. Functional conversion between A-type and delayed rectifier K+ channels by membrane lipids. *Science* 304: 265-270, 2004.**

40. **Poling JS, Vicini S, Rogawski MA and Salem N, Jr. Docosahexaenoic acid block of neuronal voltage-gated K+ channels: subunit selective antagonism by zinc. *Neuropharmacology* 35: 969-982, 1996.**

41. **Rasmusson RL, Morales MJ, Castellino RC, Zhang Y, Campbell DL and Strauss HC. C-type inactivation controls recovery in a fast inactivating cardiac K^+ channel (Kv1.4) expressed in *Xenopus* oocytes. *J Physiol* 489: 709-721, 1995.**

42. **Siddiqui RA, Harvey KA and Zaloga GP. Modulation of enzymatic activities by n-3 polyunsaturated fatty acids to support cardiovascular health. *J Nutr Biochem* 19: 417-437, 2008.**

43. **Singleton CB, Valenzuela SM, Walker BD, Tie H, Wyse KR, Bursill JA, Qiu MR, Breit SN and Campbell TJ. Blockade by N-3 polyunsaturated fatty acid of the Kv4.3 current stably expressed in Chinese hamster ovary cells. *Br J Pharmacol* 127: 941-948, 1999.**

44. Smirnov SV and Aaronson PI. Modulatory effects of arachidonic acid on the delayed rectifier K+ current in rat pulmonary arterial myocytes. Structural aspects and involvement of protein kinase C. *Circ Res* 79: 20-31, 1996.

45. Somodi S, Hajdu P, Gaspar R, Panyi G and Varga Z. Effects of changes in extracellular pH and potassium concentration on Kv1.3 inactivation. *Eur Biophys J* 37: 1145-1156, 2008.

46. Steidl JV and Yool AJ. Differential sensitivity of voltage-gated potassium channels Kv1.5 and Kv1.2 to acidic pH and molecular identification of pH sensor. *Mol Pharmacol* 55: 812-820, 1999.

47. Trimmer JS and Rhodes KJ. Localization of voltage-gated ion channels in mammalian brain. *Annu Rev Physiol* 66: 477-519, 2004.

48. Villarroel A and Schwarz TL. Inhibition of the Kv4 (*Shal*) family of transient K^+ currents by arachidonic acid. *Journal Of Neuroscience* 16: 2522-2531, 1996.

49. Warwicker J. Improved pKa calculations through flexibility based sampling of a water-dominated interaction scheme. *Protein Sci* 13: 2793-2805, 2004.

50. Xiao YF, Morgan JP and Leaf A. Effects of polyunsaturated fatty acids on cardiac voltage-activated K(+) currents in adult ferret cardiomyocytes. *Sheng Li Xue Bao* 54: 271-281, 2002.

Figure legends

Figure 1. Effect of PUFAs on wild-type $K_v1.4$

A, wild-type $K_v1.4$ current traces recorded under control conditions and in the presence of 50 μM arachidonic acid (left), 15 μM EPA (middle) and 50 μM DHA (right) (voltage pulses shown above current traces). B, current-voltage relationships for wild-type $K_v1.4$ under control conditions and in the presence of the three PUFAs. $K_v1.4$ current was measured as the peak current minus the current at the end of the pulse; the current is normalised to the peak minus end current at +90 mV under control conditions (I/I_{+90}). Means ± SEM (n=7/8) shown. pH, 7.4; extracellular K^+ concentration, 3 mM.

Figure 2. Effect of PUFAs on recovery of wild-type $K_v1.4$ from inactivation

A, superimposed wild-type $K_v1.4$ current traces during pairs of conditioning and test pulses (with different test intervals) under control conditions and in the presence of 50 μM arachidonic acid (left), 15 μM EPA (middle) and 50 μM DHA (right) (voltage pulses shown above current traces). B, time course of recovery of wild-type $K_v1.4$ from inactivation under control conditions and in the presence of the PUFAs. The peak minus end current during the test pulse (as a percentage of the peak minus end current during the preceding conditioning pulse) is plotted against the test interval. Means ± SEM (n=7/8) shown. The data are fitted with a double exponential function. pH, 7.4; extracellular K^+ concentration, 3 mM. C, wild-type $K_v1.4$ ionic current traces in the absence and presence of arachidonic acid after full recovery from inactivation (pulse interval 60 s). Voltage protocol used is presented as an inset. Current traces at +90 mV are shown. D, current-voltage relationships for wild-type $K_v1.4$ after full recovery from inactivation were constructed as previously described. Means ± SEM (n=5) shown.

Figure 3. Effect of PUFAs on C-type inactivation of K_v1.4 Δ2-146

A, Superimposed K_v1.4 Δ2-146 ionic current recordings obtained from repetitive depolarization pulses (voltage protocol used shown as an inset) under control conditions and with application of 30 μM arachidonic acid (n=6). B, An overlay of K_v1.4 Δ2-146 current recordings from depolarizing pulses of varying durations, during control condition and with application of 30 μM arachidonic acid. C, percent inactivation at the end of 4, 7.5, 15 and 30 s depolarizing pulse, with control conditions (black) and with 30 μM extracellular arachidonic acid (white). A comparison of the degree of current decay at the end of a 30 s pulse and from 4 s measurements extrapolated to 30 s showed no significant difference (NS), for both the control and arachidonic conditions. Means ± SEM (n=6). D, K_v1.4 Δ2-146 current traces recorded during perfusion of 0, 0.3, 3, 30 and 50 μM arachidonic acid, EPA and DHA (voltage pulse shown above current traces). The current traces are normalised to the peak current. E, dose-response curves for the effect of arachidonic acid (left), EPA (middle) and DHA (right) on C-type inactivation. The percentage inactivation at 4 s is plotted against the PUFA concentration (on a logarithmic scale). Means ± SEM (n=5-10) shown. The data are fitted with the Hill equation and the K_D values are shown. pH, 7.4; extracellular K^+ concentration, 3 mM.

Figure 4. Interaction between the effects of extracellular H^+ and K^+ on C-type inactivation of K_v1.4 Δ2-146

A, K_v1.4 Δ2-146 current traces recorded during perfusion of 3, 50, 100 and 200 mM K^+ solution at different pH values (voltage pulse shown above current traces). The current traces have been normalised to the peak current. B, titration curves for K_v1.4 Δ2-146 at different K^+ concentrations. The percentage inactivation at 4 s is plotted against the H^+ concentration (on

a logarithmic scale). Mean ± SEM (n=6) shown. The data are fitted with the Hill equation. C, plot of pK_a (from data in B) versus the extracellular K^+ concentration.

Figure 5. Interaction between the effects of extracellular PUFAs and H^+ on C-type inactivation of $K_v1.4$ Δ2-146

A, $K_v1.4$ Δ2-146 current traces recorded at pH 7.4 and pH 5.5 (or pH 6) with and without 30 μM arachidonic acid (top), 30 μM EPA (middle) and 30 μM DHA (bottom) (voltage pulse shown above current traces). The current traces have been normalised to the peak current. B, mean data. The top panel shows titration curves with (arachidonic acid, AA) and without (Control) 30 μM arachidonic acid. The percentage inactivation at 4 s is plotted against the H^+ concentration (on a logarithmic scale). Mean ± SEM (n=5) shown. The data are fitted with the Hill equation and pK_a values are shown. The middle and bottom panels show the mean ± SEM (n=5) percentage inactivation at 4 s with and without 30 μM EPA (middle panel) and 30 μM DHA (bottom panel) at a pH of 7.4 (filled bars) or 6 (open bars). ∗significantly different from the control at the same pH (ANOVA; $P<0.05$). Extracellular K^+ concentration, 3 mM.

Figure 6. Interaction between the effects of extracellular PUFAs and K^+ on C-type inactivation of $K_v1.4$ Δ2-146

A, $K_v1.4$ Δ2-146 current traces recorded in 3 and 100 mM K^+ with and without 30 μM arachidonic acid (top), 30 μM EPA (middle) and 30 μM DHA (bottom) (voltage pulse shown above current traces). The current traces have been normalised to the peak current. B, mean ± SEM (n=5) percentage inactivation at 4 s with and without the three PUFAs in 3 (filled bars) or 100 (open bars) mM K^+. ∗significantly different from the control at the same K^+ concentration (ANOVA; $P<0.05$). pH, 7.4.

Figure 7. Effect of PUFAs on the K_v1.4 Δ2-146 H508C and K_v1.4 Δ2-146 K532C mutant channels

A and B, K_v1.4 Δ2-146 H508C (A) and K_v1.4 Δ2-146 K532C (B) current traces recorded under control conditions and in the presence of 30 μM arachidonic acid (top), 30 μM EPA (middle) and 30 μM DHA (bottom). The currents were recorded during a 15 s voltage pulse to +60 mV from a holding potential of -80 mV. The current traces have been normalised to the peak current. The insets show the percentage inactivation at 4 s under control conditions and in the presence of the PUFA. Means ± SEM (n=5) shown. pH, 7.4; extracellular K^+ concentration, 3 mM.

Figure 8. Lipoelectric effect of arachidonic acid on wild-type K_v1.4 Δ2-146 and K_v1.4 Δ2-146 H508C channels

A and B, the voltage-dependence of activation of wild-type K_v1.4 Δ2-146 (A) and K_v1.4 Δ2-146 H508C channels (B) in the absence (open symbols) and presence of 70 μM arachidonic acid (closed symbols). The lipoelectric effect of arachidonic acid is indicated as a hyperpolarizing shift of the voltage-dependence of activation. Ionic current traces in the presence of arachidonic acid recorded from short 90 ms depolarizations from a -80 mV holding potential to +60 mV in 10 mV increments, followed by a repolarizing step to -60 mV are presented in the inset. Means ± SEM (n=11 and 5, respectively).

Figure 9. Modelling the interaction of arachidonic acid with the pore domain of K_v1.4

A, a spacefilling representation of arachidonic acid alongside two subunits of a model (31) of the K_v1.4 pore domain (S5-S6), drawn as a backbone trace. The other two subunits are omitted for ease of viewing. The selectivity filter is marked with the S1 K^+ site, and the sidechains of basic H508 and K532 (blue), and acidic D530 (red), are displayed. EC and IC

denote extracellular and intracellular. B, a structural model for arachidonic acid interaction that is consistent with the experimental data. Arachidonic acid was modelled with the hydrophobic chain along the transmembrane axis and the acidic head group protruding. The view is into the membrane extracellular face, and shows the distribution of groups radially from the central pore axis, with H508 closer in and the arachidonic acid head group further out. Note that arachidonic acid could be positioned at about this radius, whether the full $K_v1.4$ transmembrane channel (S1-S6) or just the pore domain (S5-S6) are included. The pore domain (S5-S6) is drawn as a salmon-coloured backbone, within the grey slab of membrane used in the calculations. Red and blue contours show the result of electrostatics calculation with the Finite Difference Poisson Boltzmann method (49), for a dipole balanced between a single H508 site and the S1 K^+ location, with low dielectric for the protein and membrane regions. The geometry of the dipole lobes show that a peripheral arachidonic acid interacts much more strongly with H508 than with the S1 site (and the K^+ conduction axis), supporting a model in which H508 protonation state mediates the effect of arachidonic acid. Swiss-Pdb Viewer (18) aided the preparation of this figure.

FIGURE 1

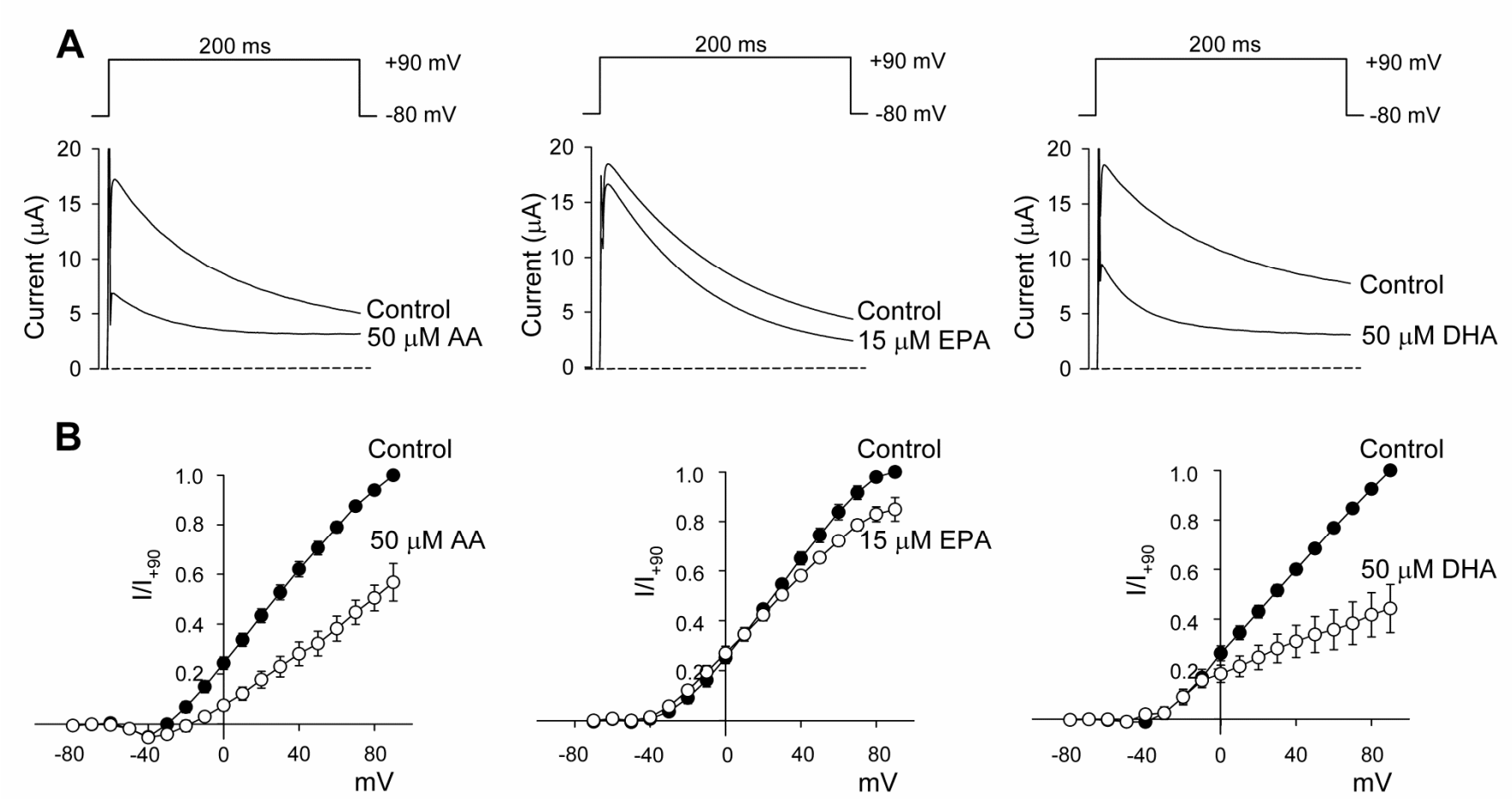
A
200 ms
+90 mV
-80 mV
Current (μA)
Control
50 μM AA
15 μM EPA
50 μM DHA
B
I/I+90
mV

FIGURE 2

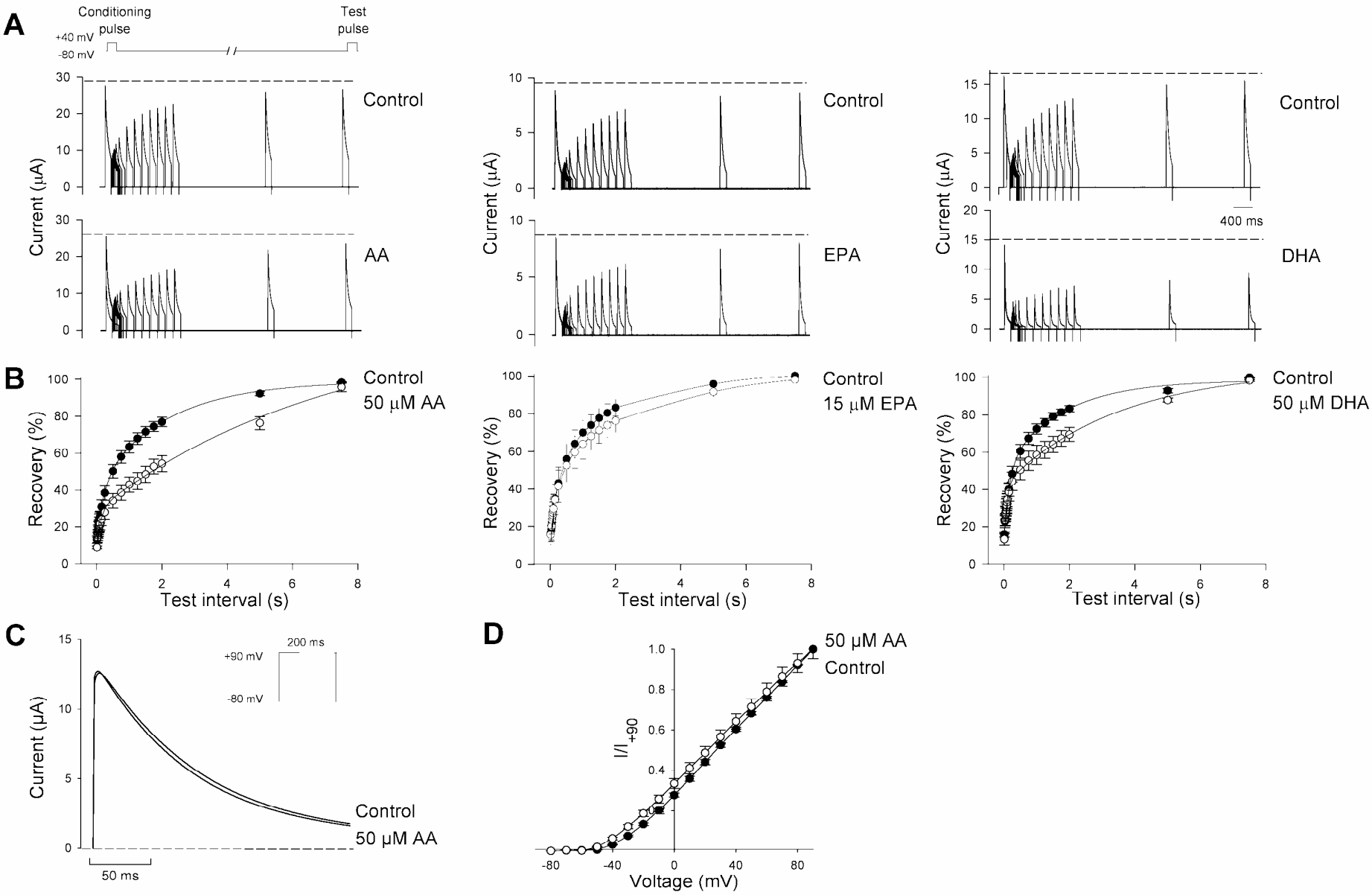
A
Conditioning pulse
Test pulse
+40 mV
-80 mV
Control
AA
EPA
DHA
400 ms
Current (μA)
B
Control
50 μM AA
15 μM EPA
50 μM DHA
Recovery (%)
Test interval (s)
C
200 ms
+90 mV
-80 mV
Control
50 μM AA
50 ms
D
50 μM AA
Control
I/I+90
Voltage (mV)

FIGURE 3

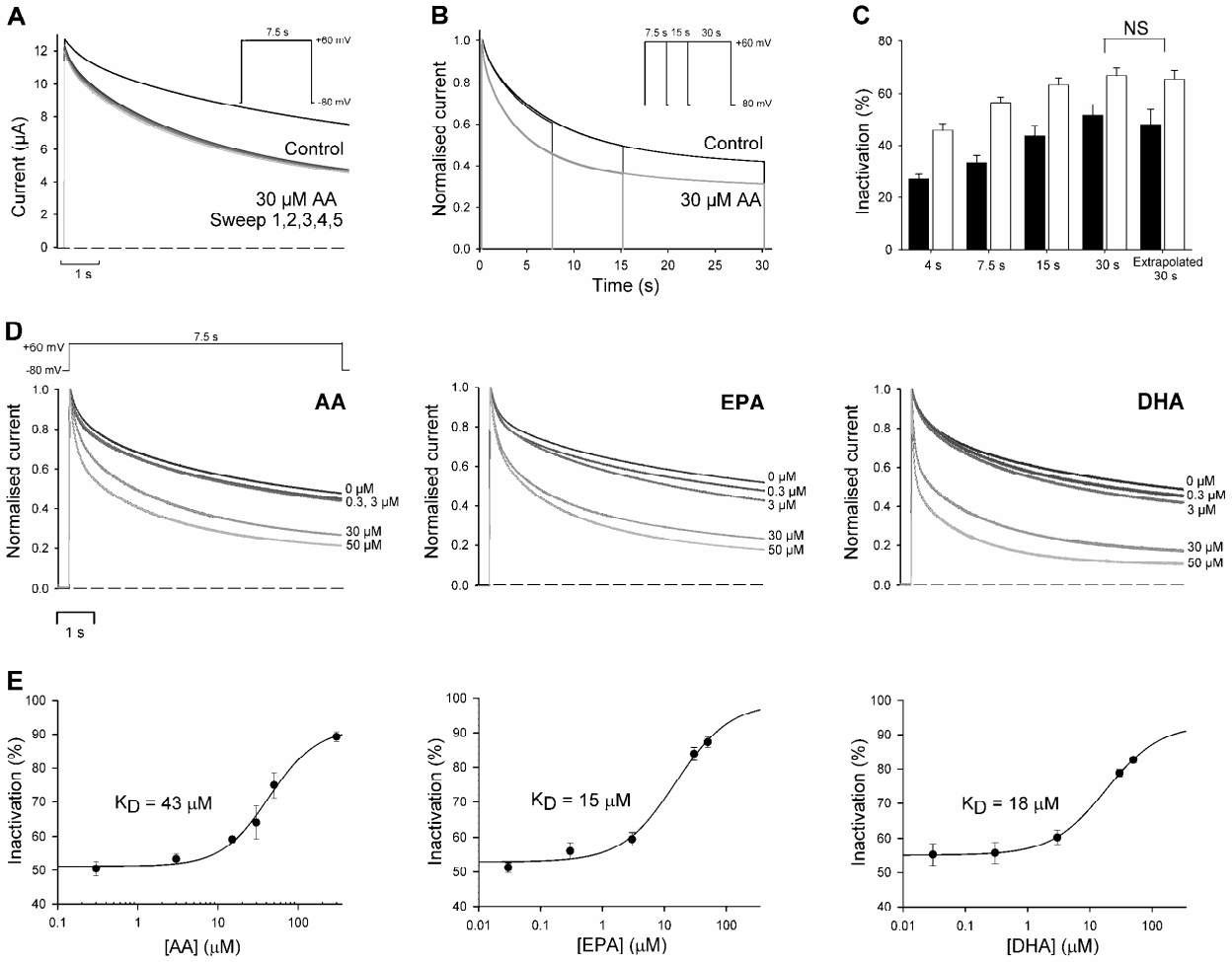
A
7.5 s
+60 mV
-80 mV
Current (μA)
Control
30 μM AA
Sweep 1,2,3,4,5
1 s
B
7.5 s 15 s 30 s
+60 mV
-80 mV
Normalised current
Control
30 μM AA
Time (s)
C
NS
Inactivation (%)
4 s
7.5 s
15 s
30 s
Extrapolated 30 s
D
+60 mV
-80 mV
7.5 s
AA
EPA
DHA
Normalised current
0 μM
0.3, 3 μM
30 μM
50 μM
0.3 μM
3 μM
1 s
E
Inactivation (%)
K_D = 43 μM
K_D = 15 μM
K_D = 18 μM
[AA] (μM)
[EPA] (μM)
[DHA] (μM)

FIGURE 4

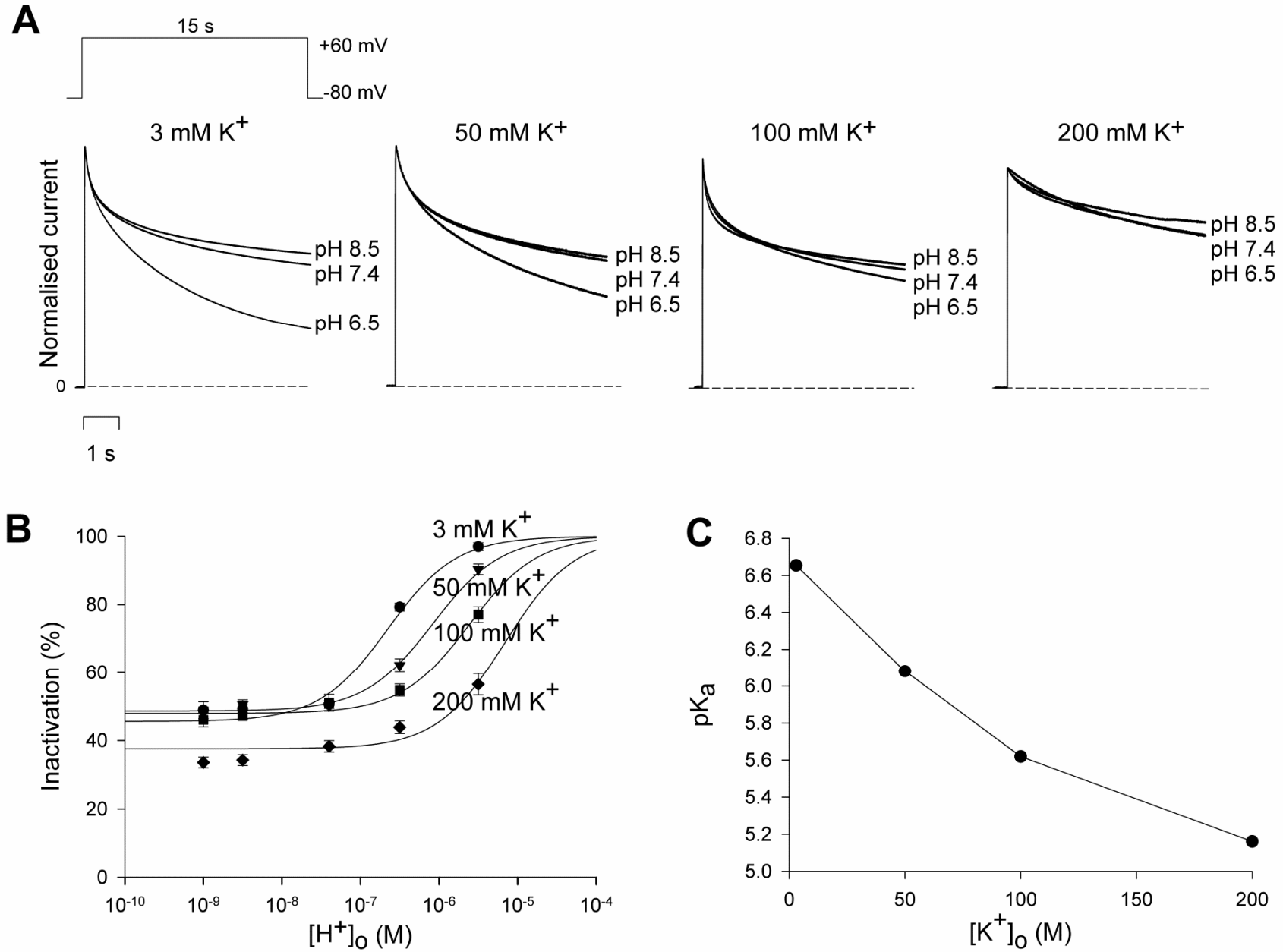
A
15 s
+60 mV
-80 mV
3 mM K+
50 mM K+
100 mM K+
200 mM K+
Normalised current
pH 8.5
pH 7.4
pH 6.5
0
1 s
B
Inactivation (%)
100
80
60
40
20
0
3 mM K+
50 mM K+
100 mM K+
200 mM K+
10-10
10-9
10-8
10-7
10-6
10-5
10-4
[H+]o (M)
C
pKa
6.8
6.6
6.4
6.2
6.0
5.8
5.6
5.4
5.2
5.0
0
50
100
150
200
[K+]o (M)

FIGURE 5

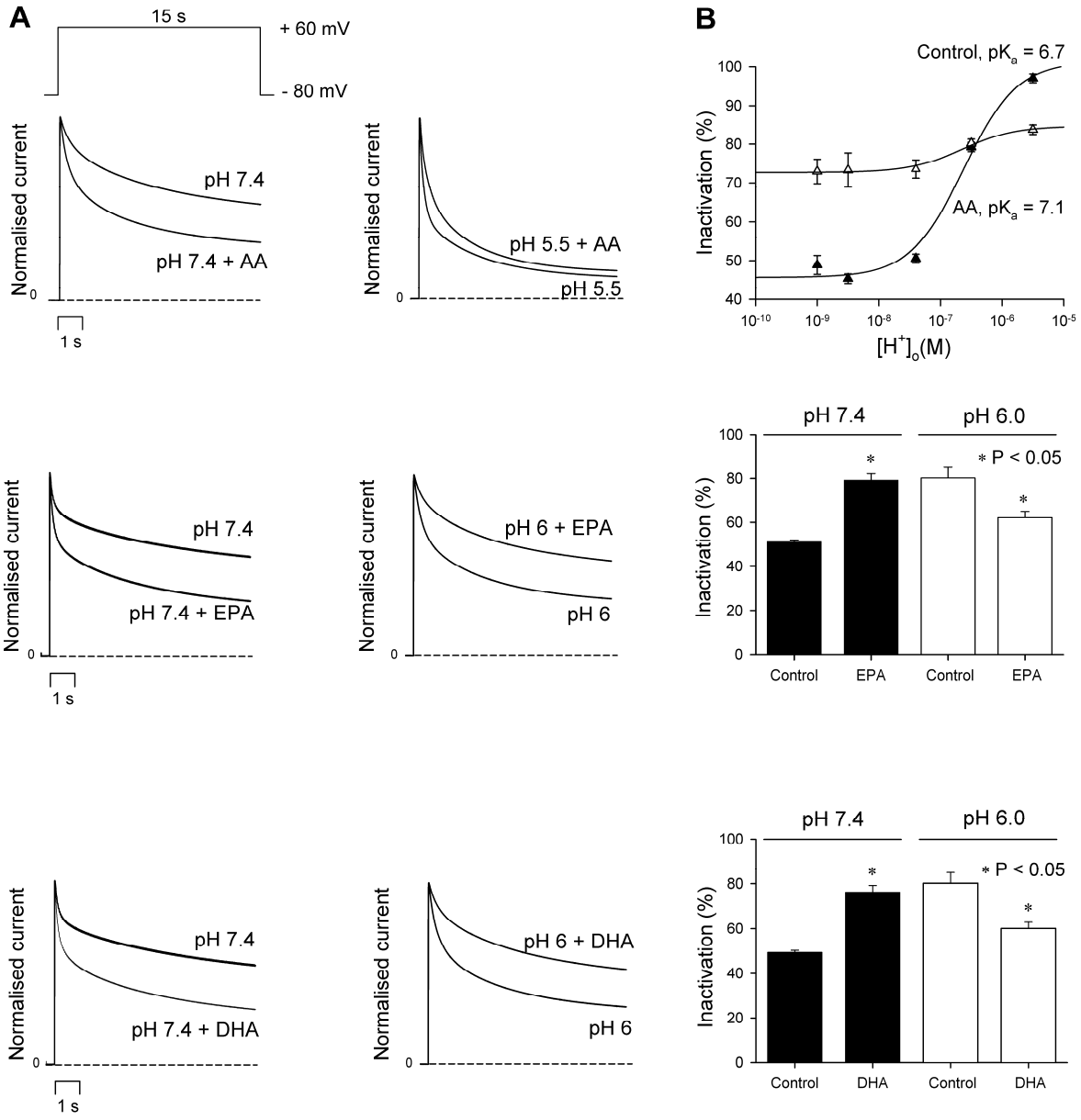
A
15 s
+ 60 mV
- 80 mV
Normalised current
pH 7.4
pH 7.4 + AA
0
1 s
Normalised current
pH 5.5 + AA
pH 5.5
0
B
Control, pK$_a$ = 6.7
AA, pK$_a$ = 7.1
Inactivation (%)
100
90
80
70
60
50
40
10^{-10}
10^{-9}
10^{-8}
10^{-7}
10^{-6}
10^{-5}
[H$^+$]$_o$(M)
Normalised current
pH 7.4
pH 7.4 + EPA
0
1 s
Normalised current
pH 6 + EPA
pH 6
0
pH 7.4
pH 6.0
* P < 0.05
Inactivation (%)
Control
EPA
Control
EPA
Normalised current
pH 7.4
pH 7.4 + DHA
0
1 s
Normalised current
pH 6 + DHA
pH 6
0
pH 7.4
pH 6.0
* P < 0.05
Inactivation (%)
Control
DHA
Control
DHA

FIGURE 6

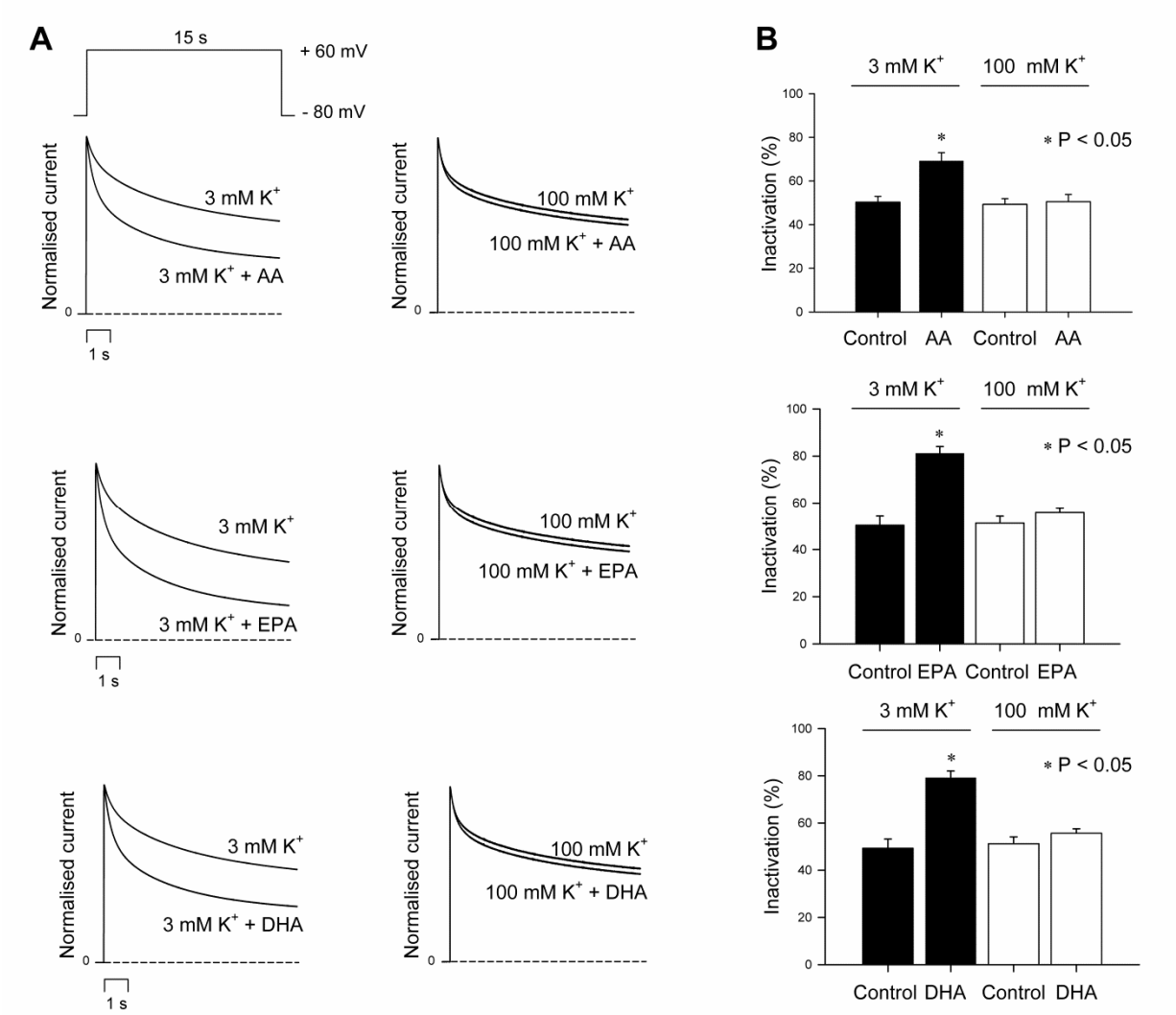
A
15 s
+ 60 mV
- 80 mV
Normalised current
3 mM K+
3 mM K+ + AA
100 mM K+
100 mM K+ + AA
3 mM K+ + EPA
100 mM K+ + EPA
3 mM K+ + DHA
100 mM K+ + DHA
0
1 s
B
3 mM K+
100 mM K+
Inactivation (%)
* P < 0.05
Control AA Control AA
Control EPA Control EPA
Control DHA Control DHA

FIGURE 7

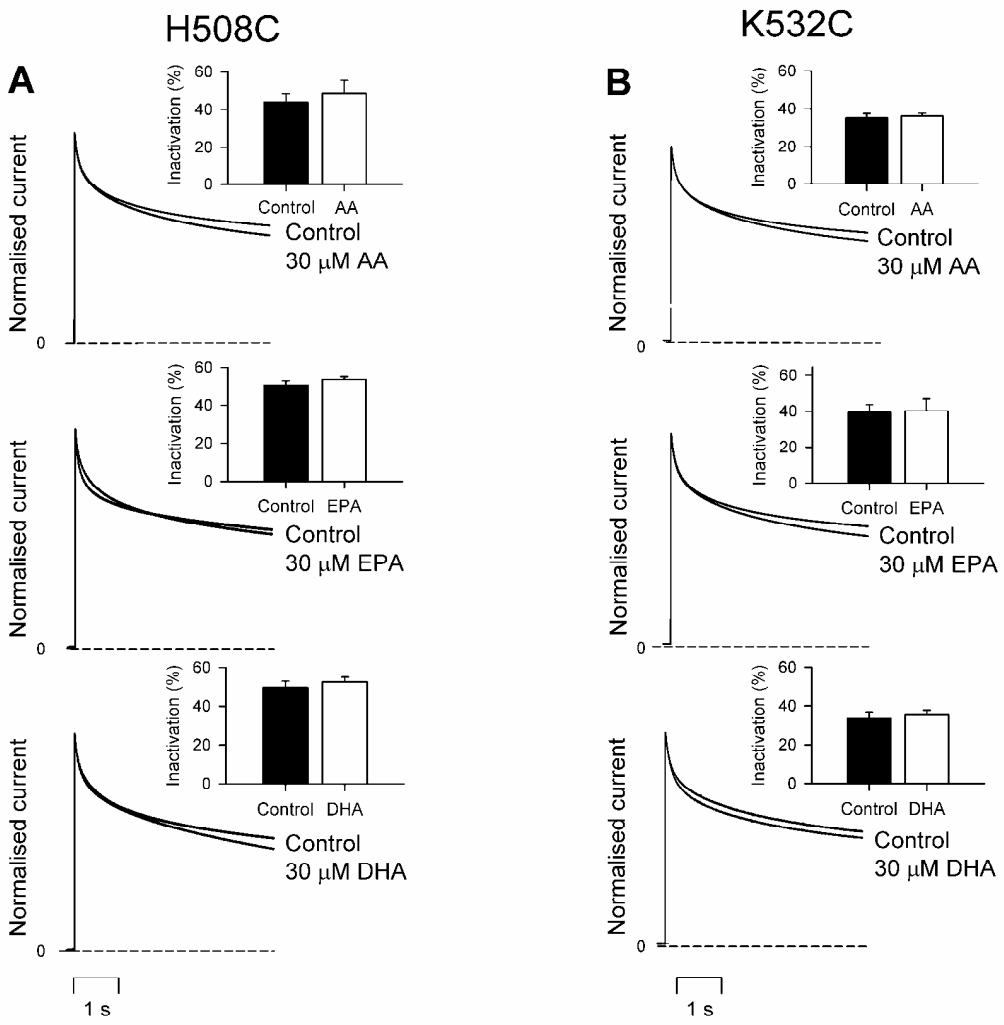
H508C
K532C
A
B
Normalised current
Inactivation (%)
60
40
20
0
Control AA
Control
30 μM AA
Control EPA
30 μM EPA
Control DHA
30 μM DHA
1 s

FIGURE 8

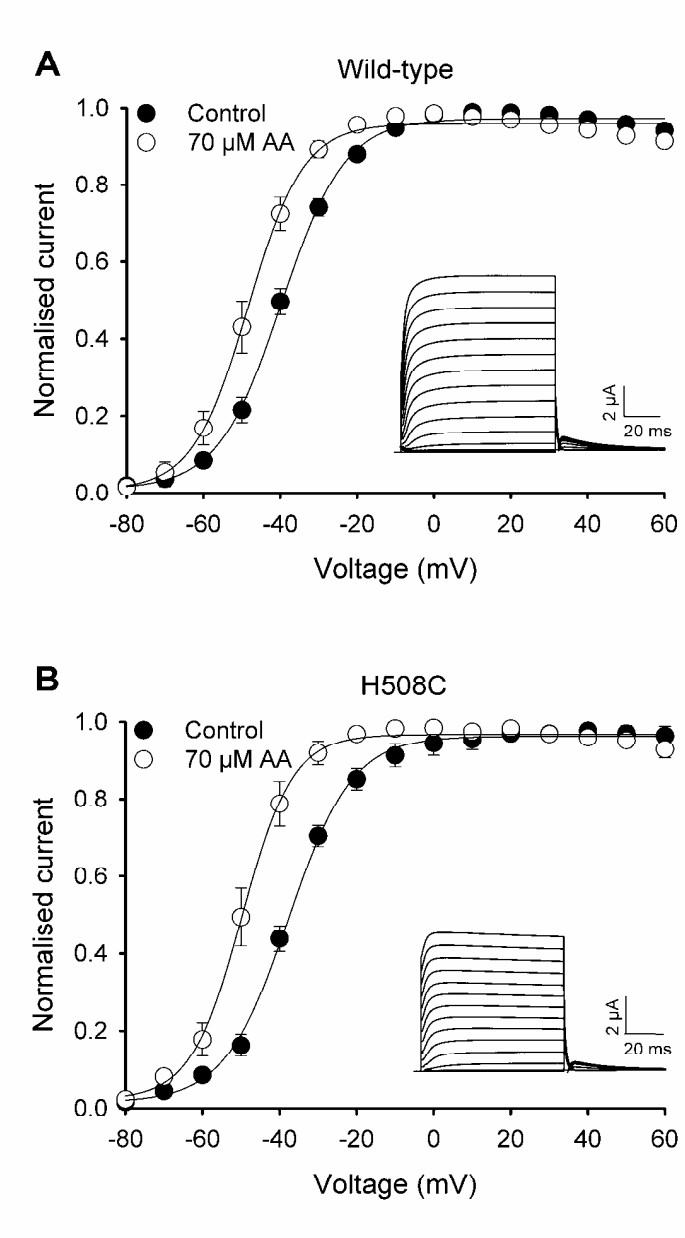
A
Wild-type
Control
70 µM AA
Normalised current
1.0
0.8
0.6
0.4
0.2
0.0
-80
-60
-40
-20
0
20
40
60
Voltage (mV)
2 µA
20 ms
B
H508C
Control
70 µM AA
Normalised current
1.0
0.8
0.6
0.4
0.2
0.0
-80
-60
-40
-20
0
20
40
60
Voltage (mV)
2 µA
20 ms

FIGURE 9